DEPARTMENT REPORT UWME-DR-201-107-1

THREE-DIMENSIONAL ELASTOPLASTIC STRESS ANALYSIS OF UNIDIRECTIONAL BORON/ALUMINUM COMPOSITES CONTAINING BROKEN FIBERS

Jayant M. Mahishi
Donald F. Adams

October 1982

TECHNICAL REPORT
NASA-Lewis Research Center
Grant No. NSG-3217

Approved for Public Release: Distribution Unlimited

COMPOSITE MATERIALS RESEARCH GROUP
DEPARTMENT of MECHANICAL ENGINEERING
University of Wyoming Laramie, Wyoming 82071

DEPARTMENT REPORT
UWME-DR-201-107-1

THREE-DIMENSIONAL ELASTOPLASTIC STRESS ANALYSIS OF UNIDIRECTIONAL BORON/ALUMINUM COMPOSITES

JAYANT M. MAHISHI
DONALD F. ADAMS

OCTOBER 1982

TECHNICAL REPORT
NASA-LEWIS RESEARCH CENTER
GRANT NO. NSG-3217

COMPOSITE MATERIALS RESEARCH GROUP
MECHANICAL ENGINEERING DEPARTMENT
UNIVERSITY OF WYOMING
LARAMIE, WYOMING 82071

1. Report No.	2. Government Accession No.	3. Recipient's Catalog No.
4. Title and Subtitle Three-Dimensional Elastoplastic Stress Analysis of Unidirectional Boron/Aluminum Composites		5. Report Date October 1982 6. Performing Organization Code
7. Author(s) Jayant M. Mahishi and Donald F. Adams		8. Performing Organization Report No. UWME-DR-201-107-1 10. Work Unit No.
9. Performing Organization Name and Address Composite Materials Research Group University of Wyoming Laramie, WY 82071		11. Contract or Grant No. NSG-3217 13 Type of Report and Period Covered Technical Report
12. Sponsoring Agency Name and Address NASA-Lewis Research Center 21000 Brookpark Road Cleveland, OH 44135		14. Sponsoring Agency Code

15. Supplementary Notes

Program Monitor: Dr. J.A. DiCarlo
Materials Science Branch

16. Abstract

A three-dimensional elastoplastic finite element micromechanical model has been developed to study the state of stress around a broken fiber surrounded by unbroken fibers in a unidirectional composite. A boron/aluminum composite consisting of 50 percent by volume of fibers in a square array and subjected to an axial loading is taken as a specific example. This loading in the fiber direction is applied in small increments, by prescribing increments of boundary displacement, until the first failure occurs. The effect of reduced material properties of the aluminum matrix material at elevated temperature is also studied. The results are presented in the form of stress contours and stress-strain plots.

17. Key Words (Suggested by Author(s))	18. Distribution Statement
Boron/Aluminum Composites Metal Matrix Composites Micromechanics Analysis 3D Finite Element Analysis	Unclassified, Unlimited

19. Security Classif. (of this report)	20. Security Classif. (of this page)	21. No. of Pages	22. Price*
Unclassified	Unclassified	32	

* For sale by the National Technical Information Service, Springfield, Virginia 22161

Preface

This fourth annual Technical Report represents the final report of a study conducted under NASA-Lewis Grant NSG-3217. The NASA-Lewis Technical Monitor since the inception of this grant has been Dr. J.A. DiCarlo of the Materials Science Branch.

This study was performed within the Composite Materials Research Group at the University of Wyoming. The Principal Investigator was Dr. Donald F. Adams, Professor of Mechanical Engineering. Mr. J.M. Mahishi, Ph.D. student in Mechanical Engineering, performed the work contained herein, as part of his research assistantship duties within the Composite Materials Research Group.

TABLE OF CONTENTS

SECTION 1

INTRODUCTION

The present report is the fourth and final annual report under a NASA-Lewis sponsored project to study the energy absorption mechanisms active during crack propagation in metal-matrix composites.

A micromechanical approach was adopted to study the initiation and propagation of matrix cracks emanating from broken fibers in unidirectional composites. A literature review of the general topic of micromechanical analyses of unidirectional composites as related to the present study was included in the first-year report [1]. During the first two years, simple two-dimensional longitudinal and transverse cross section models were used to study the influence of broken fibers on the inelastic stress distribution. An existing elastoplastic, generalized plane strain finite element micromechanics analysis [2-4], with crack propagation capability based on the general procedure developed earlier by Adams [5-8], was used. Work on an axisymmetric model consisting of a single broken fiber embedded in a circular sheath of matrix material was also initiated during the second year period [9]. The axisymmetric model was primarily developed to facilitate a planned experimental verification of the analytical work, since it is relatively simple to fabricate and test a single-fiber composite.

During the third year, the axisymmetric model was further refined, to include a constant displacement boundary condition during an increment of crack propagation [10]. The new boundary condition permitted a substantial amount of slow and stable crack growth, as opposed to the almost immediate catastrophic failure observed in the case of the earlier constant stress

boundary condition model. The energy absorbed during stable crack growth was calculated and the concept of crack growth resistance curves was used to determine the point of crack instability. The crack growth resistance curves (K_R-curves or R-curves), for various fiber volume contents, are given in Reference [11]. The third-year report also provides information required for a possible experimental verification of the analysis, viz, the aspect ratio of the specimen to be used, the predicted crack opening displacement as a function of applied load, the variation of surface longitudinal and circumferential strains with applied loads, etc. It is also possible to generate the R-curves from the experimentally measured crack opening displacement (COD), using the compliance method described in Reference [12].

During the present fourth-year effort, a three-dimensional model has been developed, to further study the influence of broken fibers on the inelastic stress distribution in a more rigorous manner. A three-dimensional elastoplastic finite element program recently developed by the Composite Materials Research Group [13] was modified to include a 20-node quadratic isoparametric element and a stress smoothing technique [14] for accurate prediction of node point stresses. A fiber volume content of 50 percent, with the fibers assumed to be packed in a regular square array, is used as an example. The analysis accounts for temperature-dependent material properties by expressing the properties as coefficients of second-order polynomials. The effect of reduced material properties at two elevated temperatures, viz, 400°F and 600°F, on the local stress distributions, and also on predicted first failure, is studied. Results are presented in the form of plots of stress contours, and composite stress-strain curves.

SECTION 2

THREE-DIMENSIONAL FINITE ELEMENT MODEL

The two-dimensional longitudinal and transverse models previously considered [1,9], even though providing some understanding of the influence of broken fibers on the stress state in the matrix and in the neighboring continuous fibers, do not adequately represent the true three-dimensional nature of actual unidirectional, fiber-reinforced composites. On the other hand, the axisymmetric model of a single broken fiber embedded in a sheath of matrix material [10,11] only represents an idealized model composite, and does not take into account the influence of the array of neighboring continuous fibers. A three-dimensional model consisting of broken fibers and continuous fibers is obviously a better alternative. Analytical approaches such as the continuum three-dimensional "material model" formulation adopted by Goree and Gross [15] incorporate a number of restrictive assumptions in order to reduce the complexity of the formulation. With the rapidly increasing capabilities of digital computers, the use of three-dimensional finite element models such as in the present analysis appears to be a much more powerful approach.

Figure 1 shows a typical cross section of a unidirectional composite with fibers packed in a regular square array. Because of the assumed periodicity, it is possible to isolate a repeating cell, such as the one containing a single broken fiber surrounded by an array of continuous fibers indicated in Figure 1. This single repeating cell consists of 25 percent of broken fibers, as shown in Figure 1. Making use of symmetry, only one quadrant of the repeating cell actually need be modeled.

The three-dimensional elastoplastic finite element program developed

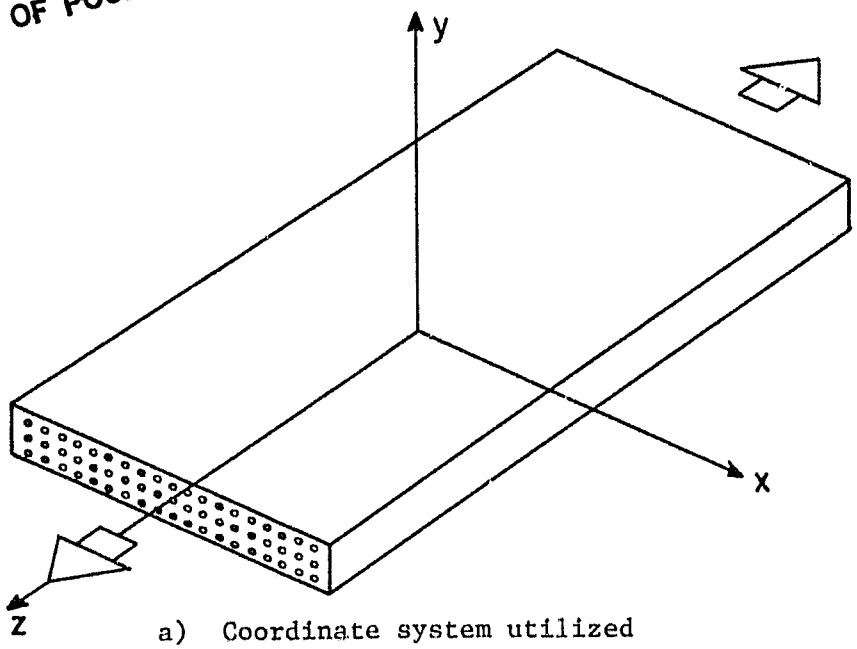

a) Coordinate system utilized

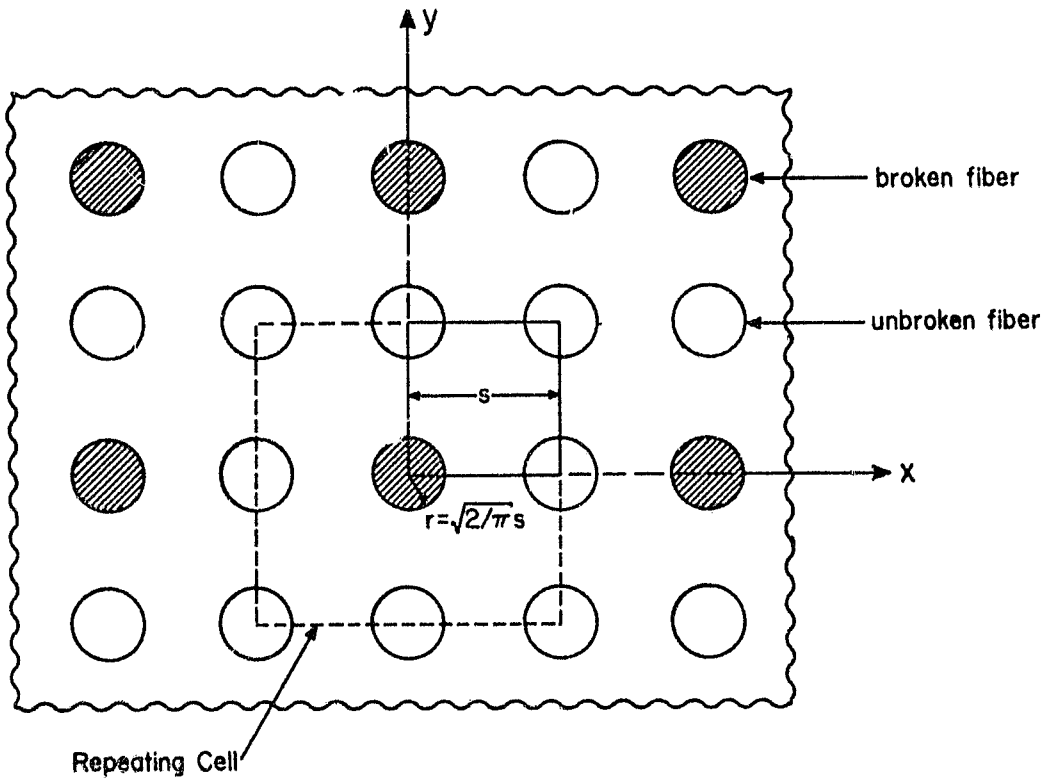

b) Square array fiber packing (50 volume percent) with repeating cell indicated

Figure 1. Unidirectional Composite Model

by Monib and Adams [13] has been modified as part of the present study to include a 20-node quadratic, isoparametric element [16]. The quadratic isoparametric element, which can model the circular boundary of the cross section of a fiber exactly, requires fewer elements than the large number of linear elements that might have been required to fit the curved boundary of the fiber. In addition, the quadratic isoparametric element is better able to represent the steep stress gradients in the matrix near the broken fiber.

The finite element model representing one quarter of the repeating cell of Figure 1 is shown in Figure 2. The model is 7½ fiber diameters long in the z-direction. A total of 144 elements were utilized, resulting in 938 nodes. The model also incorporates the double-node concept [10] at the junction of the broken fiber and the surrounding matrix, in order to represent the actual conditions of total discontinuity of the fiber at the break, while retaining the continuity of the matrix material at the same point. In addition, in the present model the double nodes are constrained to have identical displacements in the x and y directions. In the previous axisymmetric model [10,11], this condition of constrained displacement for the double nodes was not satisfied.

The displacement boundary conditions for a quadrant of the repeating cell shown in Figure 1b require that the displacements of all nodes on the righthand vertical boundary be uniform, and the displacements of all nodes on the upper horizontal boundary be uniform. This complex boundary condition has been achieved in the present three-dimensional model by assigning the same global degree of freedom to all nodes that are required to have the same displacements. The resulting three-dimensional model, by including the constrained boundary conditions discussed above, represents

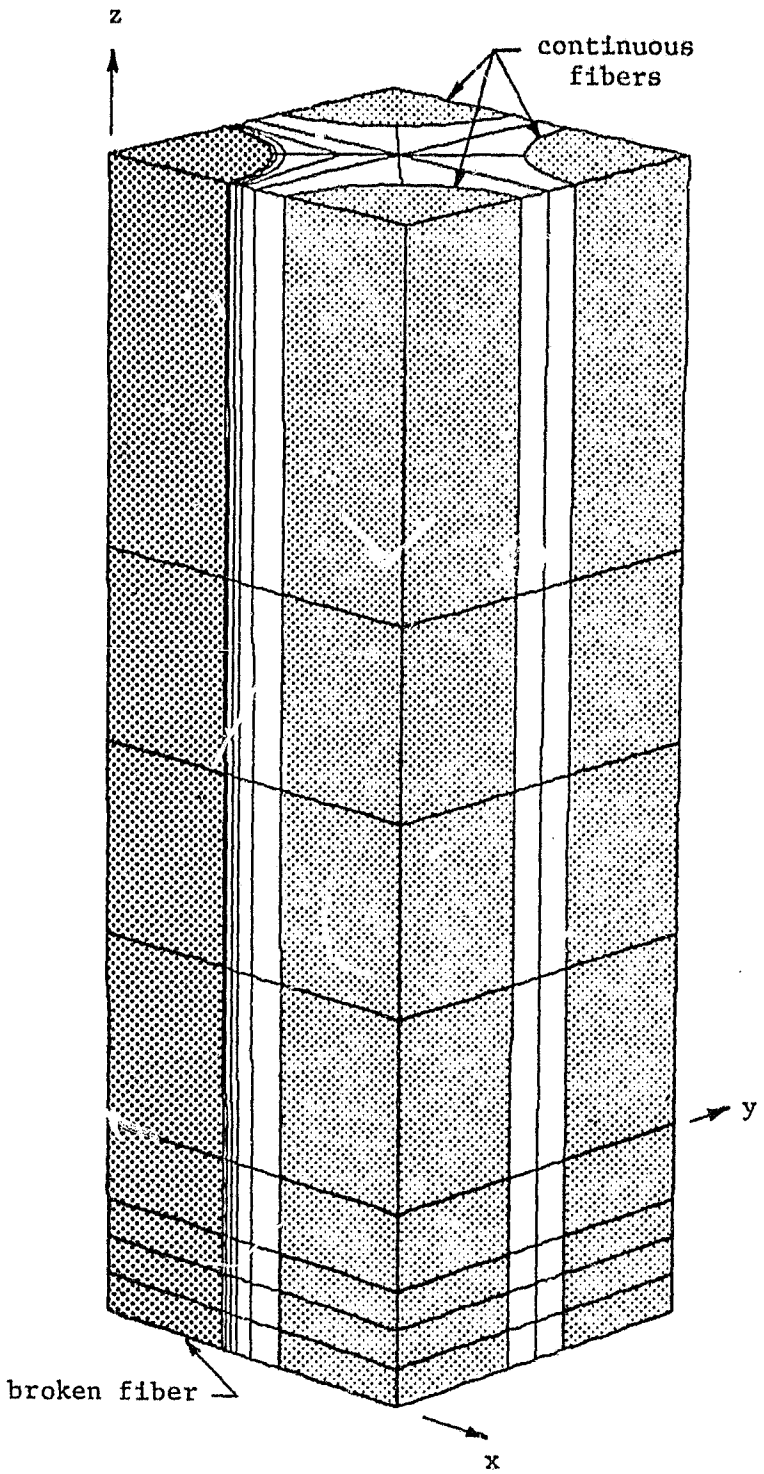

a) Isometric view

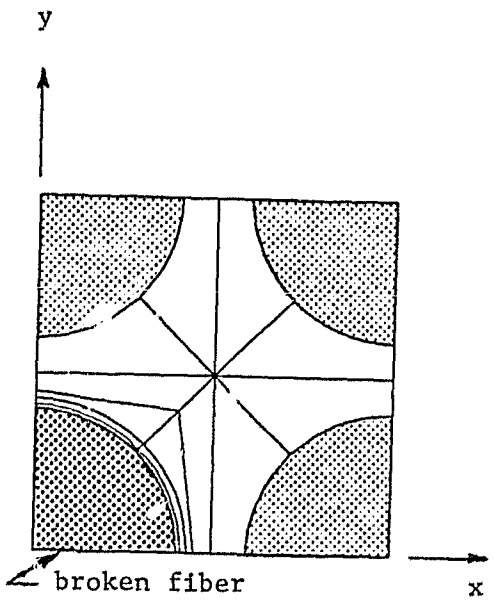

b) Cross section at z = 0

Figure 2. Finite Element Model of One Quadrant of the Repeating Cell.

the micromechanics model without any simplifying assumptions being required.

SECTION 3

MATERIAL PROPERTIES

The boron fibers utilized in the present boron/aluminum composites have been modeled as linearly elastic materials to failure, with isotropic strength and stiffness properties. The temperature-dependent mechanical and physical properties given in References [17,18] for boron fibers as commercially supplied have been expressed for present purposes in second-order polynomial form, i.e.,

$$P(T) = C_1T^2 + C_2T + C_3 \tag{1}$$

where P(T) represents the functional material property of interest, and T is the temperature. Figures 3 and 4 (taken from Reference [18]) show the variation of normalized fiber axial modulus and normalized ultimate tensile strength with temperature.

The matrix material utilized in the present analysis was 6061-T6 aluminum alloy. The temperature-dependent elastoplastic material properties of the 6061-T6 aluminum alloy were obtained from Reference [19]. The elastoplastic behavior of the aluminum alloy is accounted for in the finite element analysis by curve-fitting via a Richard-Blacklock three-parameter equation [20]. Figure 5 shows the stress-strain curve of the 6061-T6 aluminum alloy at 75°F [19]. Figures 6,7,8 and 9 show the variations of the mechanical and physical properties with temperature, these data also being taken from Reference [19].

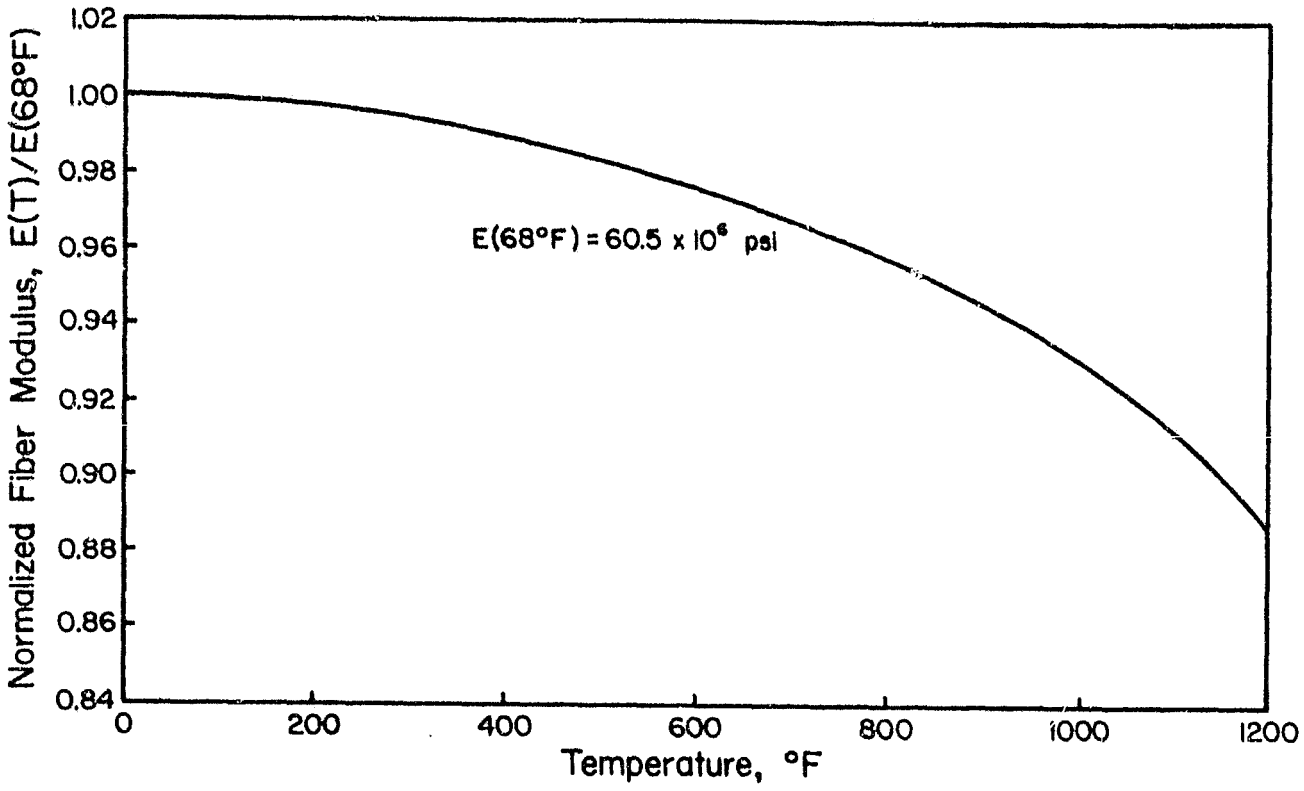

Figure 3. Temperature Dependence of Axial Young's Modulus of Boron Fibers, Normalized With Respect to Room Temperature Modulus [18].

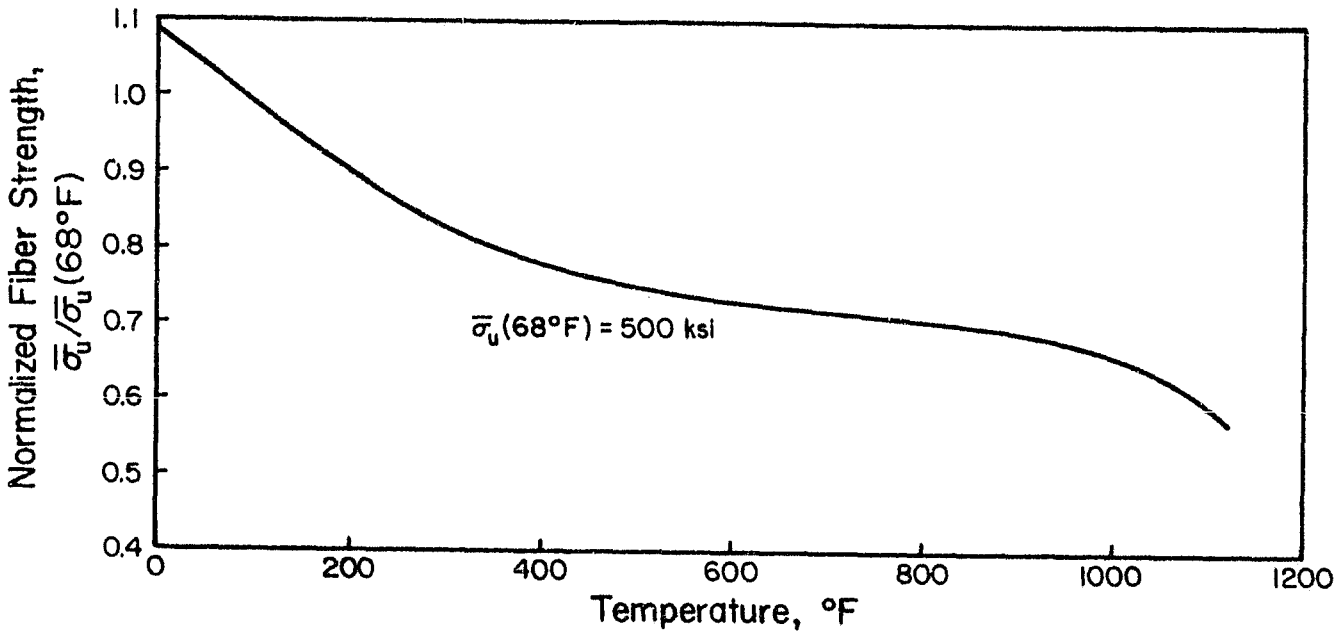

Figure 4. Temperature Dependence of Ultimate Tensile Strength of As-Produced Boron Fibers, Normalized With Respect to Room Temperature Strength [18].

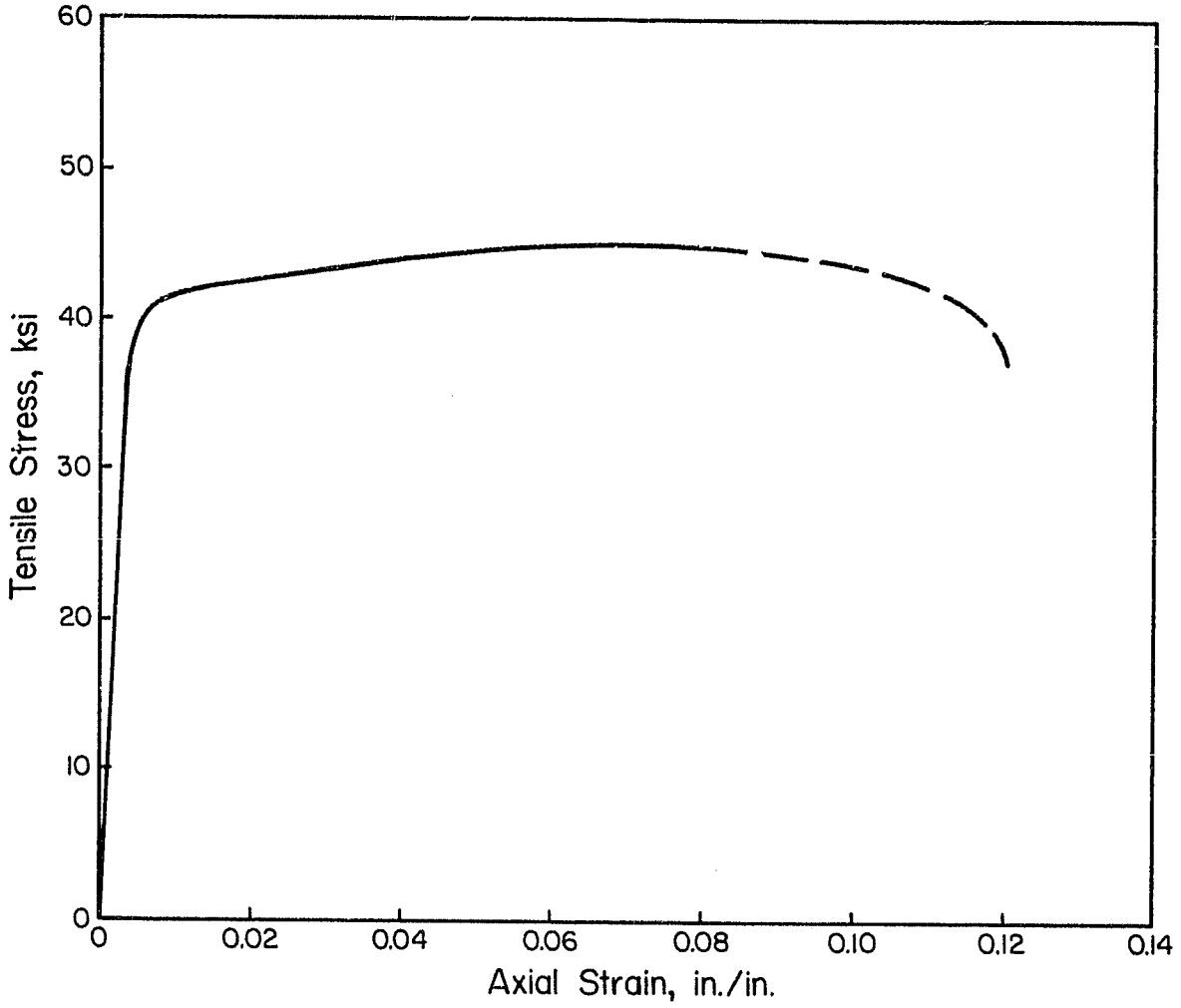

Figure 5. Typical Tensile Stress-Strain Curve (Full-Range) for 6061-T6 Aluminum Alloy (Sheet) at Room Temperature (75°F).

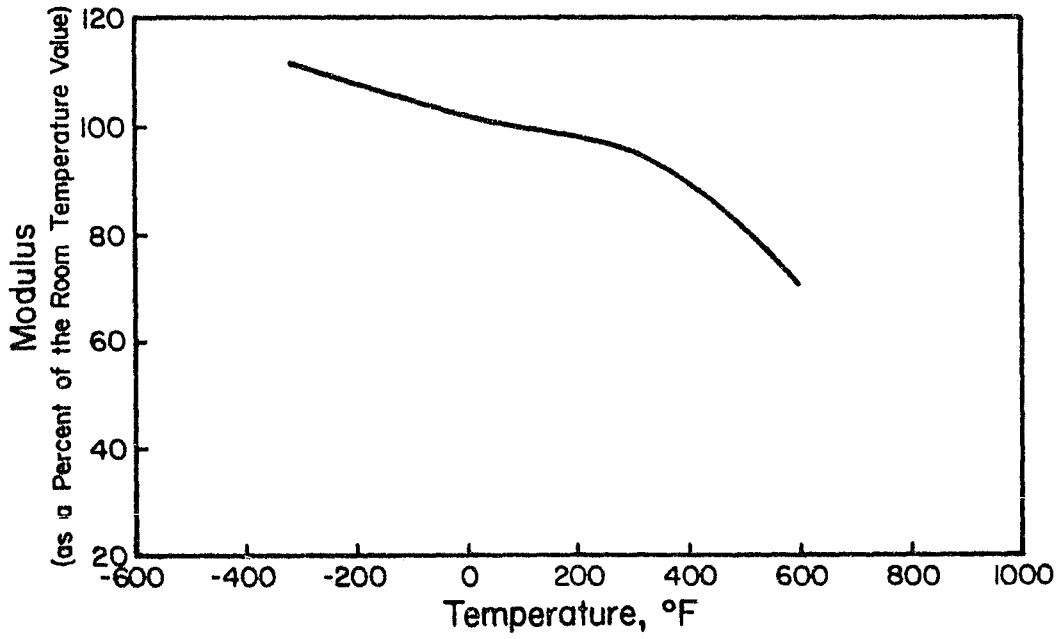

Figure 6. Effect of Temperature on the Tensile and Compressive Moduli of 6061 Aluminum Alloy.

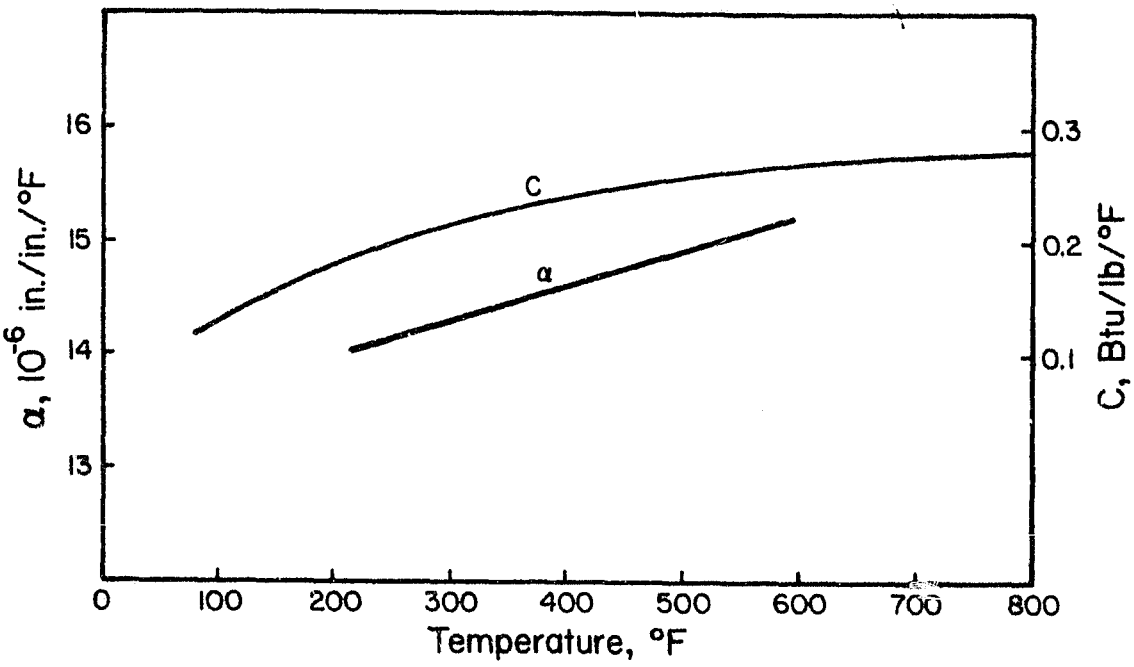

Figure 7. Effect of Temperature on the Thermal Expansion and Heat Capacity Properties of 6061 Aluminum.

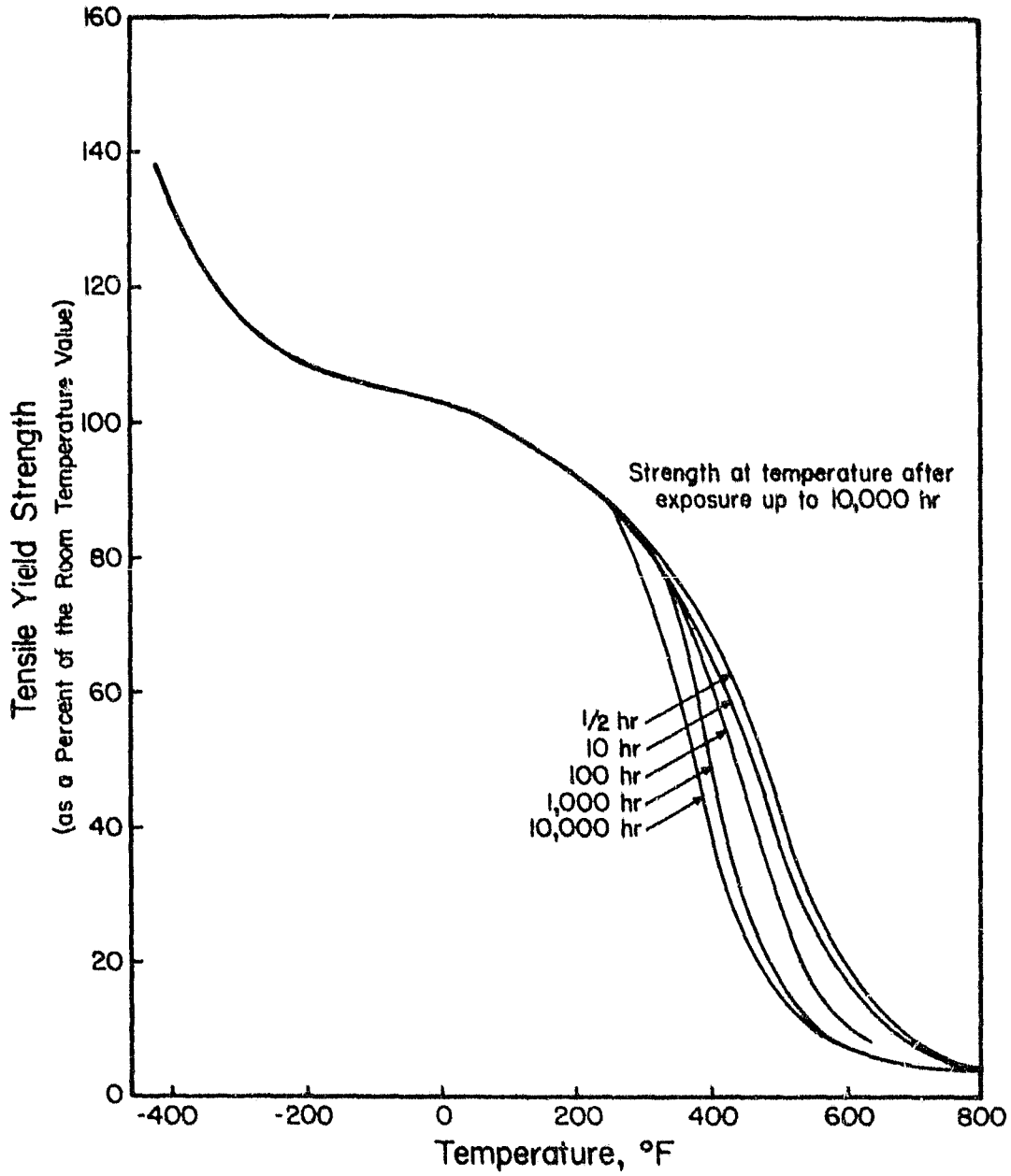

Figure 8. Effect of Temperature on the Tensile Yield Strength of 6061-T6 Aluminum Alloy.

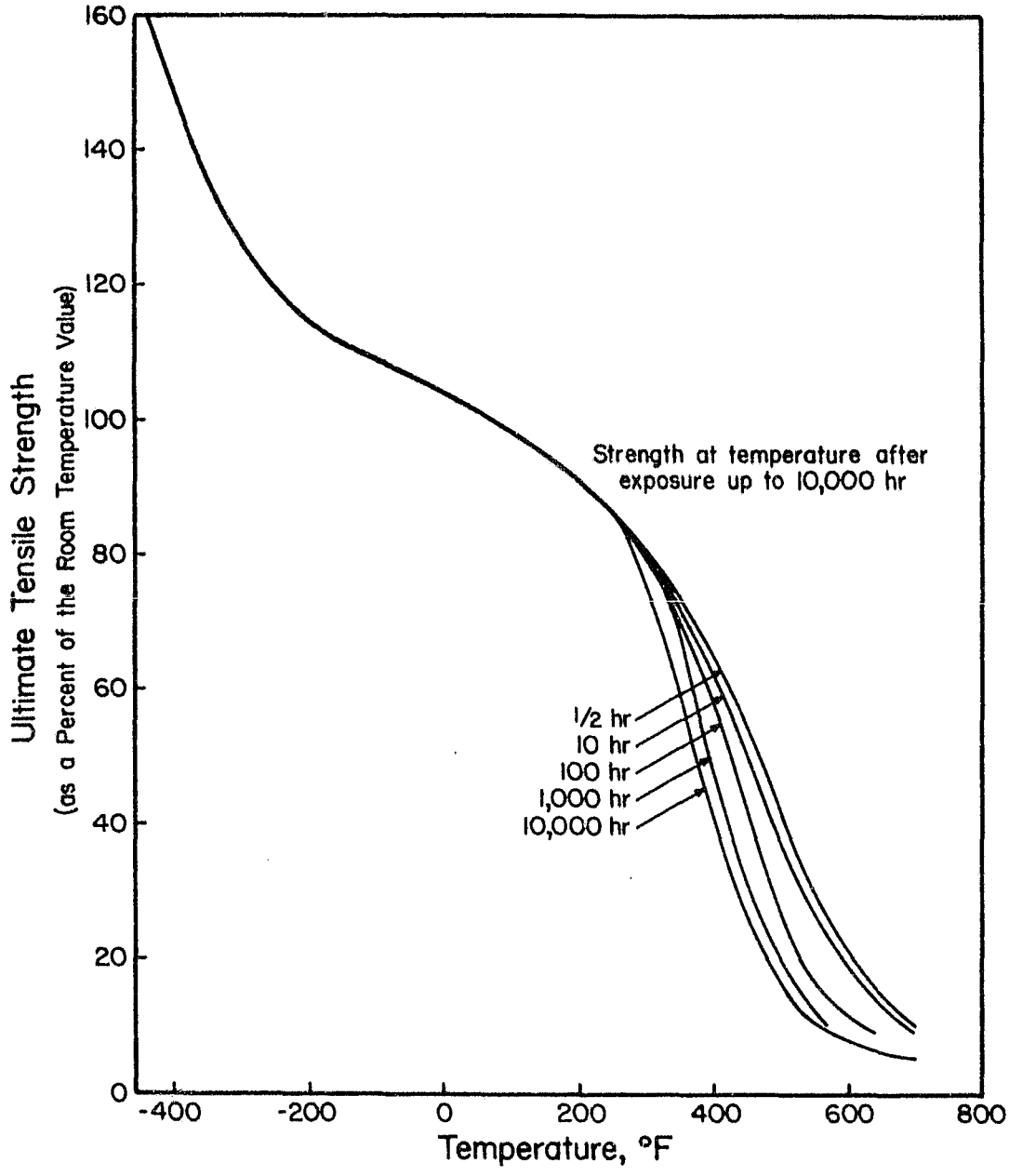

Figure 9. Effect of Temperature on the Ultimate Tensile Strength of 6061-T6 Aluminum Alloy.

SECTION 4

NUMERICAL RESULTS

The stress distributions around a broken fiber in a boron/aluminum composite, the constituent materials having the properties presented in Section 3, are given in this section. The assumed 50 percent fiber volume content finite element model shown in Figure 2 was used.

Figures 10 and 11 are the contour plots of axial normal stress (σ_{zz}) and longitudinal shear stress (τ_{xz}), respectively, in the elastic range in the matrix on three different cross sections of the composite model. The stresses have been normalized with respect to the applied average axial stress ($\bar{\sigma}_z$). Figures 10 and 11 indicate that the elastic stress concentration due to the fiber break is confined to a very localized region, and that an essentially uniform stress state is regained within a distance of two fiber diameters from the fiber break along the fiber axis. The maximum longitudinal stress concentration near the fiber break is 4.2, compared to 7 in the case of the single broken fiber axisymmetric model [10]. Although much of this difference is undoubtedly due to the fact that two different physical models are being compared, some of the difference is probably also related to the fact that a much finer finite element grid was used in modeling the single fiber geometry. More work remains to be done before totally valid comparisons can be made.

Figure 12 shows the effect of a fiber break on the elastic stress distribution in the neighboring continuous fibers. The fibers diagonally opposite to the broken fiber in the square array seem to be less affected than those adjacent to the broken fibers.

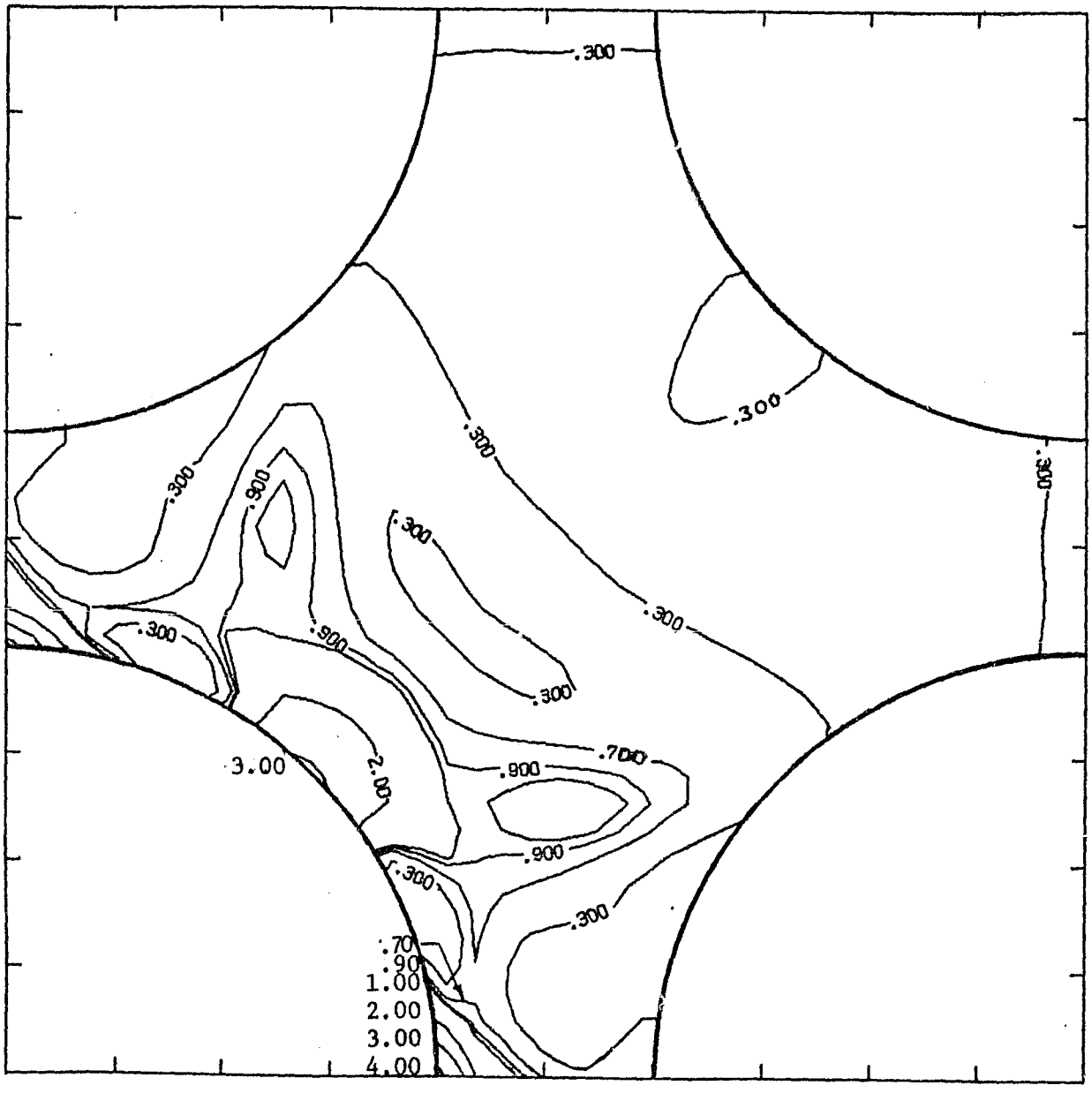

a) x-y plane at z = 0

Figure 10. Contour Plots of Normalized Axial Stress σ_{zz} (Normalized With Respect to the Applied Average Axial Stress $\bar{\sigma}_z$), in the Aluminum Matrix on Three Different Cross Sections.

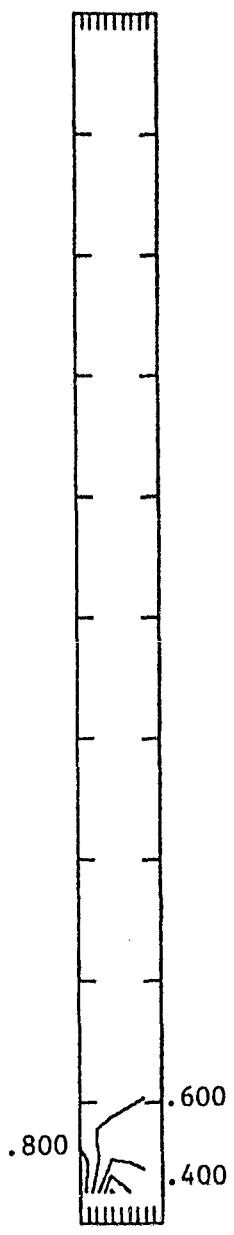

b) x-z plane at y = 0

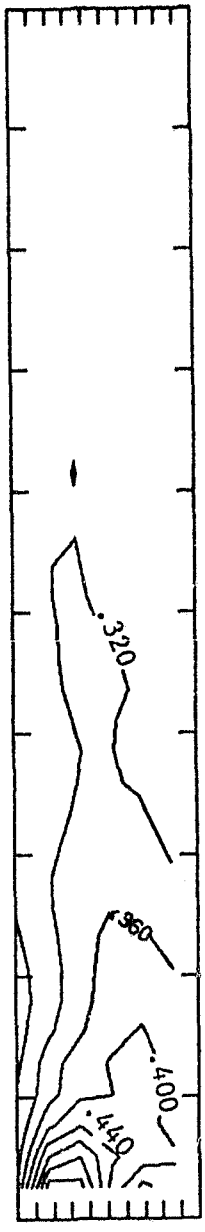

c) vertical plane at 45° to x-z plane

Figure 10. Continued.

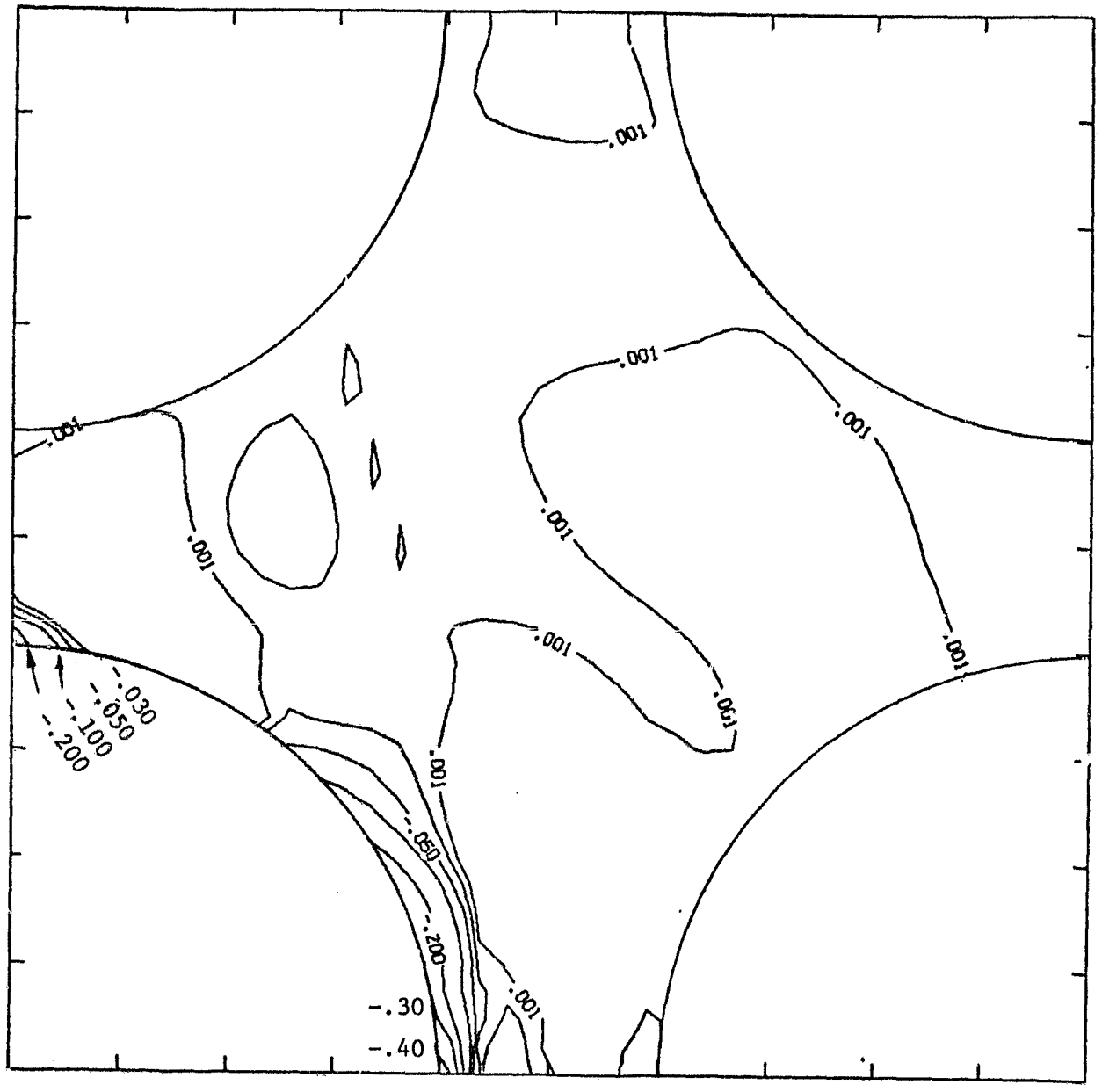

a) x-y plane at z = 0

Figure 11. Contour Plots of Normalized Longitudinal Shear Stress τ_{xz} (Normalized With Respect to the Applied Average Axial Stress $\bar{\sigma}_z$) in the Aluminum Matrix on Three Different Cross Sections.

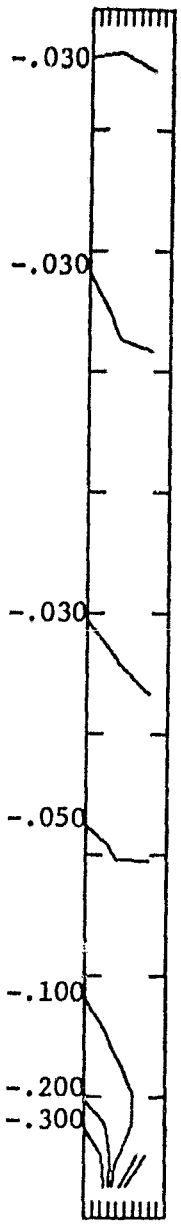

b) x-z plane at y = 0

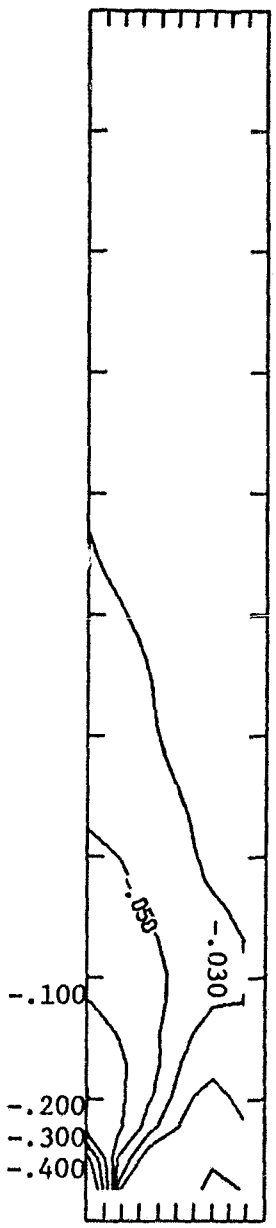

c) vertical plane at 45° to x-z plane

Figure 11. Continued.

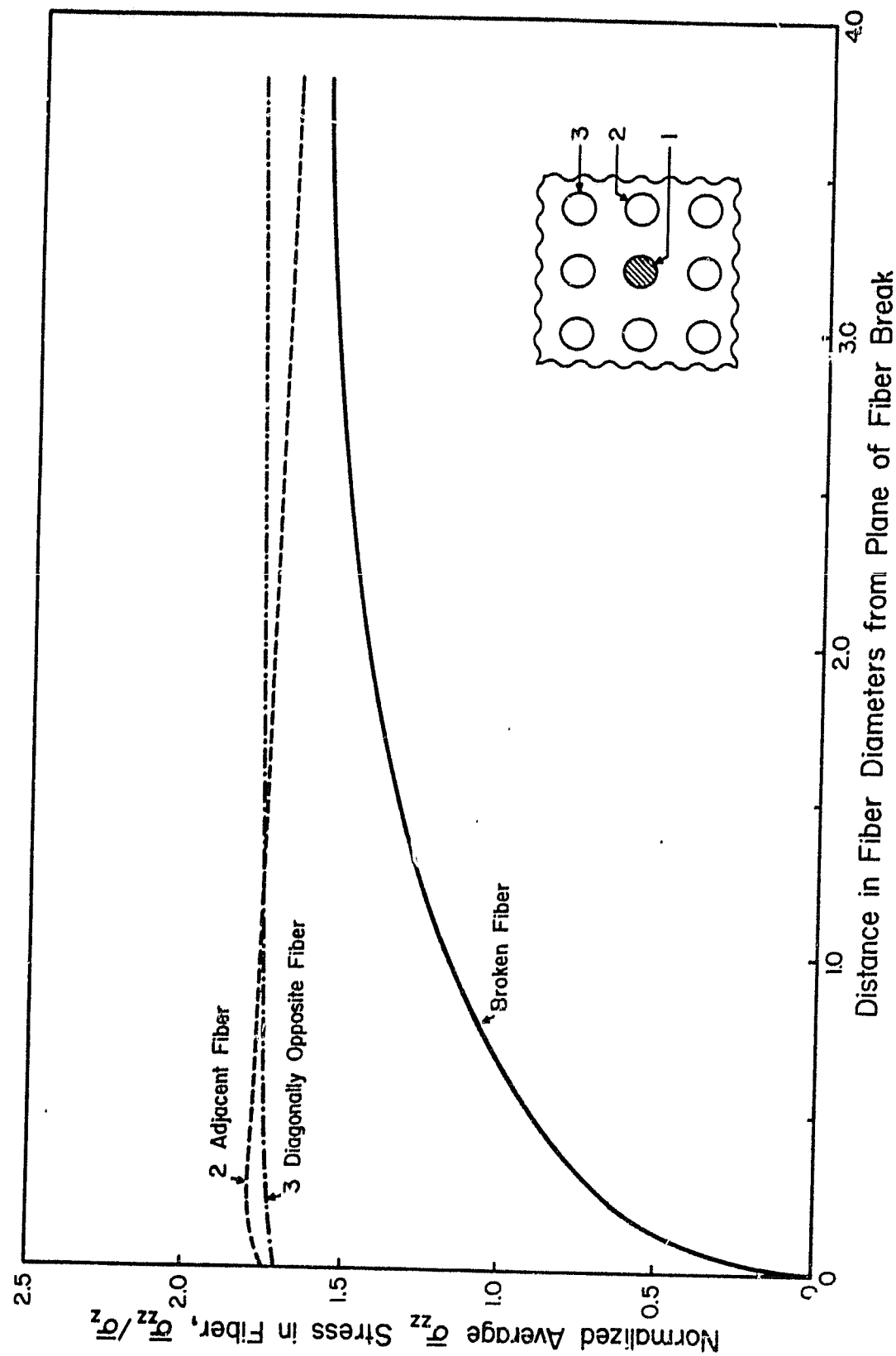

Figure 12. Normalized Average Axial Stresses in Fibers (Normalized With Respect to Average Applied Composite Axial Stress) Versus Distance From Fiber Break.

In Figure 13, the elastic longitudinal shear stress along the broken fiber-aluminum matrix interface is plotted as a function of distance in fiber diameters from the fiber break. Comparison is also made with respect to the longitudinal shear stress variation along the fiber-matrix interface in the case of a single broken fiber in a sheath of matrix material (using data from Reference [10]).

The analysis and associated computer program was extended into the inelastic range of matrix material response also, to demonstrate this capability. Figure 14 is a plot of the normalized axial stress contours throughout the matrix, for an applied axial loading on the composite model of 11,200 psi. This corresponds to the loading increment just prior to that which initiated first failure. Since the yield stress of the aluminum matrix at room temperature is 36,000 psi (see Figure 5), a stress contour of 3.2 or higher (36,000 ÷ 11,200) indicates material in the inelastic range. Thus, at this applied stress, only a small volume of matrix material has yielded (see Figure 14a), on the plane of the fiber break in the regions between the closest fiber spacings. On the other hand, the highest stress contour indicated in Figure 14a, i.e., 4, corresponds to a stress of 44,800 psi, which is only slightly less than the 45,000 psi tensile ultimate strength of the aluminum matrix (see Figure 5). That is, for the 6061-T6 aluminum alloy being modeled, the inelastic range of material response is small.

To continue the loading beyond that indicated in Figure 14, a crack initiation and propagation capability in the analysis will be required.

A comparison of Figures 10 and 14, the stresses in both plots having been normalized by dividing by their respective applied stresses, indicates that the local concentration of stress at the fiber break has spread

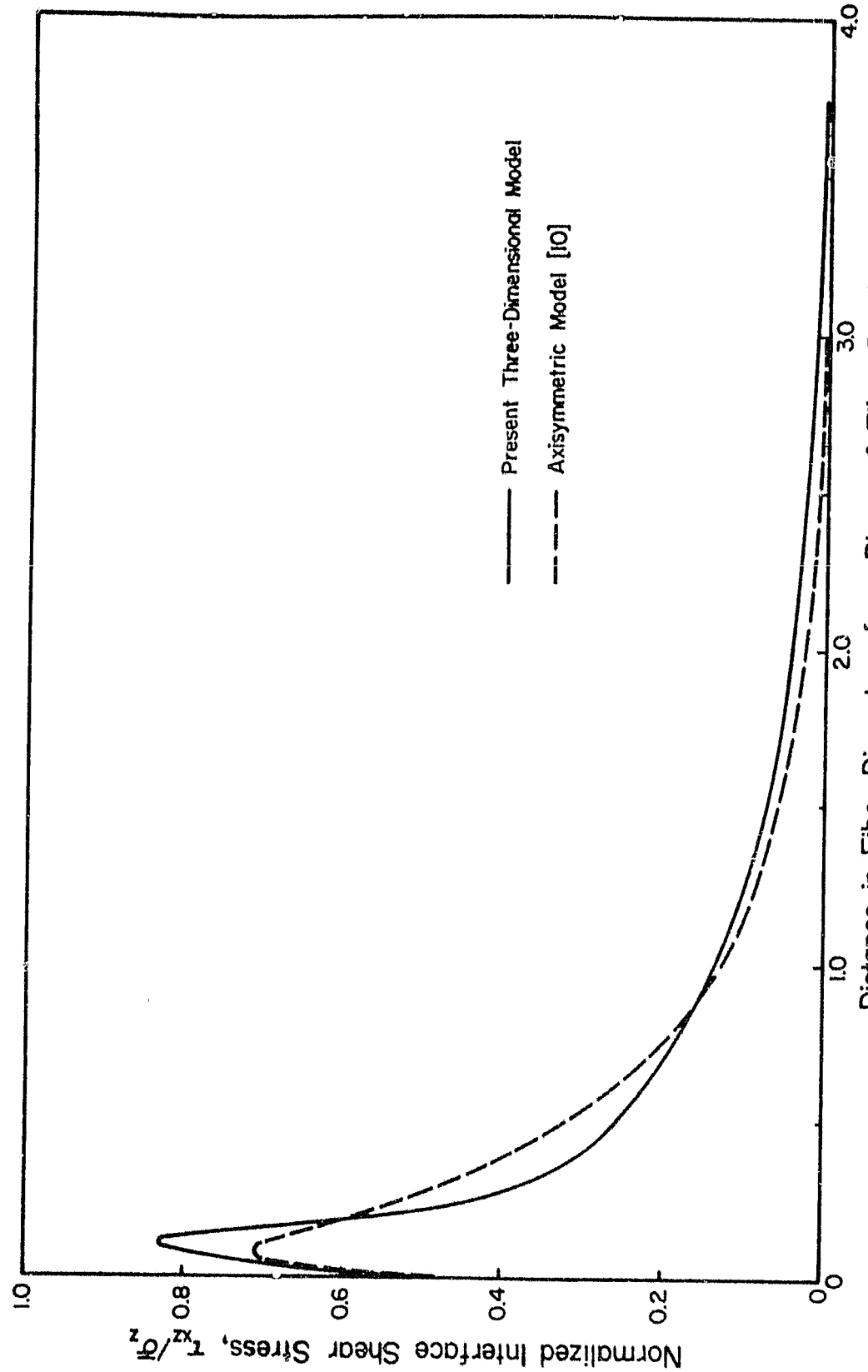

Figure 13. Variation of Longitudinal Shear Stress in the Aluminum Matrix Along the Interface of the Broken Boron Fiber (Normalized With Respect to the Average Applied Axial Stress).

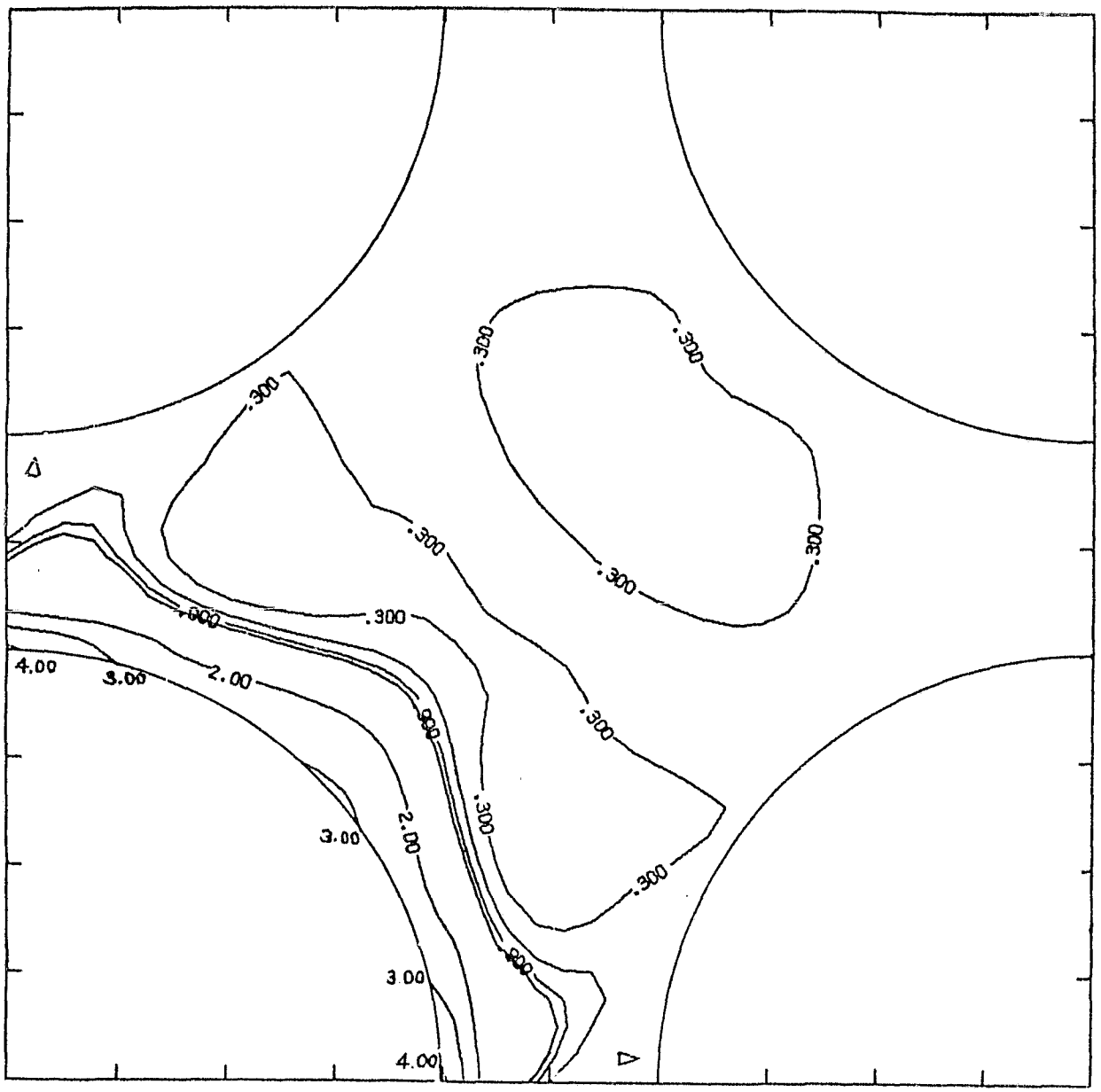

a) x-y plane at z=0

Figure 14. Contour Plots of Normalized Axial Stress σ_{zz} (Normalized With Respect to the Applied Average Axial Stress, $\bar{\sigma}_z$ = 11200 psi) in the Aluminum Matrix on Three Different Cross Sections.

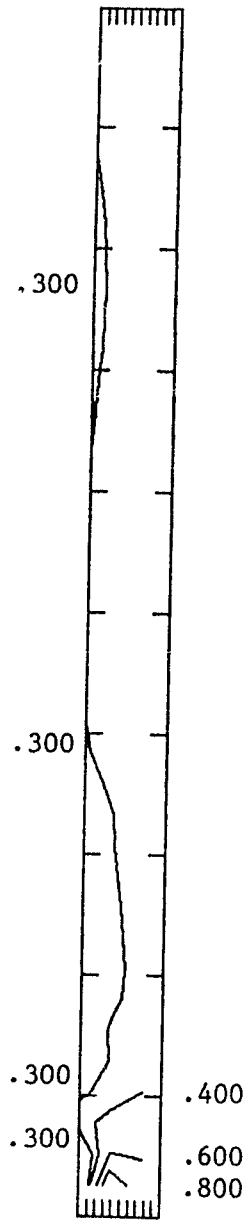

b) x-z plane at y = 0

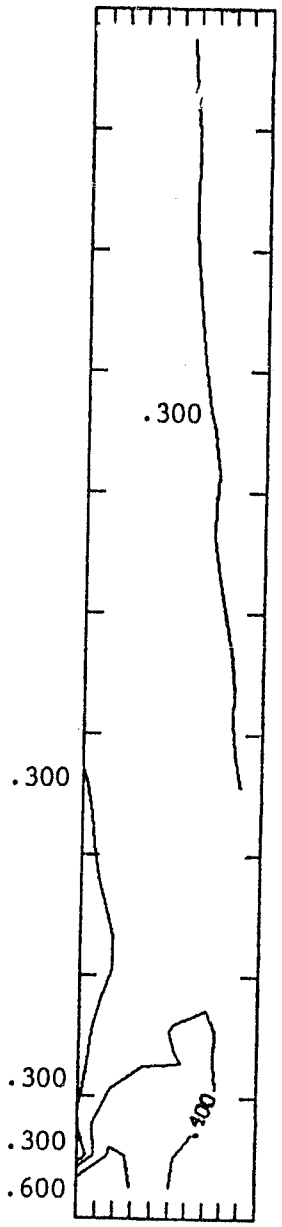

c) vertical plane at 45° to x-z plane

Figure 14 Continued.

slightly at the higher applied stress (Figure 14), due to the redistribution of loading caused by the yielding. This is as expected, of course, and is one of the benefits of stressing the ductile matrix composite into the inelastic range.

Results in the inelastic range similar in format to those of Figures 12 and 13 representing the elastic range were plotted also. However, the results were not significantly different, again because of the very limited extent of yielding prior to first failure. Thus, these plots have not been included here.

Much more work remains to be done in applying the present three-dimensional finite element analysis to practical problems. The one example presented here is intended only as a limited demonstration of the capability of such an analysis.

The original purpose of including the temperature-dependent material properties was to study the influence of residual thermal stresses due to the fabrication process. However, during the first few trial computer runs it was found that the nodes near the fiber break were failing during the cooling from the elevated fabrication temperature condition. The three-dimensional finite element computer program in its present form halts when the first node fails. The situation was similar when the model was used to study the thermomechanical response of the boron/aluminum composite at elevated temperature, as indicated in Figure 15. Obviously a crack propagation scheme similar to that in the axisymmetric finite element model [9-11] is required, to permit mechanical or thermal loading beyond first failure. A crack propagation scheme based upon the principle of maximum energy release rate is now under development.

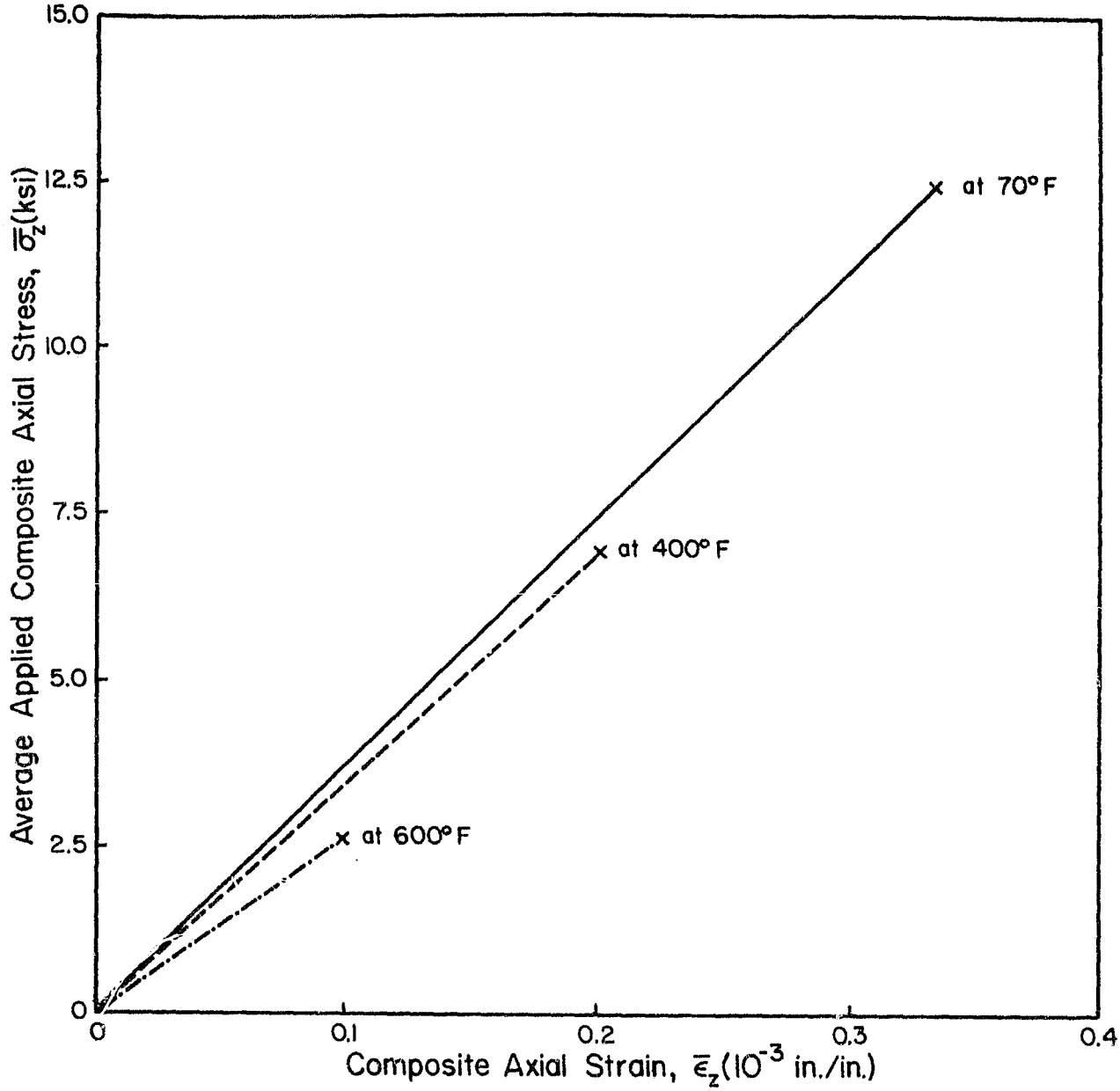

Figure 15. Predicted Axial Stress-Strain Response (to First Failure) of a Boron/Aluminum Composite Containing Broken Fibers, at Different Temperatures.

In order to demonstrate how much the reduction in constituent material properties at elevated temperature affects the strength of the boron/aluminum composite containing broken fibers, the three-dimensional finite element computer program was used to apply an axial loading at two constant elevated temperatures, viz, 400°F and 600°F. Figure 15 shows the stress-strain response of the boron/aluminum broken-fiber model composite at room temperature, 400°F and 600°F. The stress plotted in Figure 15 is the average composite stress corresponding to an applied axial strain.

SECTION 5

CONCLUSIONS AND SUGGESTIONS FOR FUTURE WORK

The three-dimensional, elastoplastic, finite element micromechanics model presented in this report is more effective in determing the true stress state around broken fibers in metal-matrix composites than the two-dimensional longitudinal and transverse models previously reported in References [1-9]. There are no major simplifying assumptions made in deriving this three-dimensional model. When the addition of a crack propagation scheme is completed, the analysis will be ideal for studying the basic energy absorption mechanisms in composites. A crack propagation scheme based on the maximum energy release rate is in progress and will be available for such studies soon.

The analysis can be extended in future studies to include different types of flaws in composites, in addition to pre-existing fiber breaks. For example, the number and severity of experimentally determined weak sites along the fiber length can be modeled. Similarly, sites of weaker bonding between fibers and matrix can also be included. These future studies should result in a more realistic failure model, in which a number of cracks initiate as fiber breaks at weak sites, and propagate steadily along the fiber-matrix interface or across the matrix. These cracks may subsequently coalesce and grow in an unstable manner, leading to final fracture. The thermal residual stresses induced due to fabrication processes, and also the thermomechanical response of the composite at elevated temperatures, at attempted in the present study, can also be included in any future analysis. It will also be relatively straightforward to include in the analysis any inherent fabrication

residual stresses in the fibers [21].

While the analytical models are continuing to be improved and extended, a parallel experimental study needs to be initiated at some stage, to support the analytical predictions. The axisymmetric model was primarily developed for this purpose. The use of the axisymmetric model to analyze polymer-matrix composites [22,23] should simplify the experimental work, as the optical transparency of the polymer matrix will permit direct observation of the crack propagation, and measurement of crack opening displacements, whereas the metal matrix composite would require an X-ray technique, or some similar process.

In summary, the recently developed three-dimensional finite element analysis and computer program [13] used in the present study appears to offer significant opportunities for use in the study of fracture mechanisms in composite materials. While much additional work needs to be done, both in the further development of the finite element model, and in the generation of supporting experimental data, the potential of the approach has been clearly demonstrated.

REFERENCES

1. Murphy, D.P. and Adams, D.F., "Energy Absorption Mechanisms During Crack Propagation in Metal Matrix Composites," Report UWME-DR-901-103-1, Department of Mechanical Engineering, University of Wyoming, Laramie, Wyoming, October 1979.

2. Miller, A.K. and Adams, D.F., "Micromechanical Aspects of the Environmental Behavior of Composite Materials," Report UWME-DR-701-111-1, Department of Mechanical Engineering, University of Wyoming, Laramie, Wyoming, January 1977.

3. Adams, D.F. and Miller, A.K., "Hygrothermal Microstresses in a Unidirectional Composite Exhibiting Inelastic Material Behavior," Journal of Composite Materials, Vol. 11, No. 3, July 1977, pp. 285-299.

4. Miller, A.K. and Adams, D.F., "Inelastic Finite Element Analysis of a Heterogeneous Medium Exhibiting Temperature and Moisture Dependent Material Properties," Fibre Science and Technology, Vol. 13, No. 2, March-April 1980, pp. 135-153.

5. Adams, D.F., "High Performance Composite Materials for Vehicle Construction; An Elastoplastic Analysis of Crack Propagation in a Unidirectional Composite," Report R-1070-PR, The Rand Corporation, Santa Monica, California, March 1973.

6. Repnau, T. and Adams, D.F., "A Finite Element Computer Program for Elastoplastic Analysis of Crack Propagation in a Unidirectional Composite," Report R-1392-PR, The Rand Corporation, Santa Monica, California, October 1973.

7. Adams, D.F., "Elastoplastic Crack Propagation in a Transversely Loaded Unidirectional Composite," Journal of Composite Materials, Vol. 8, No. 1, January 1974, pp. 38-54.

8. Adams, D.F., "A Micromechanical Analysis of Crack Propagation in an Elastoplastic Composite Material," Fibre Science and Technology, Vol. 7, No. 4, October 1974, pp. 237-256.

9. Adams, D.F. and Murphy, D.P., "Analysis of Crack Propagation as an Energy Absorption Mechanism in Metal Matrix Composites," Report UWME-DR-101-102-1, Department of Mechanical Engineering, University of Wyoming, Laramie, Wyoming, February 1981.

10. Adams, D.F. and Mahishi, J.M., "Micromechanical Predictions of Crack Propagation and Fracture Energy in a Single-Fiber Boron/Aluminum Model Composite", Report UWME-DR-201-101-1, Department of Mechanical Engineering, University of Wyoming, Laramie, Wyoming, February 1982.

11. Mahishi, J.M. and Adams, D.F., "Micromechanical Predictions of Crack Initiation, Propagation and Crack Growth Resistance in Boron/Aluminum Composites", to appear in the Journal of Composite Materials, Vol. 16, 1982.

12. Gagger, S. and Broutman, L.J., "Crack Growth Resistance of Random Fiber Composites", Journal of Composite Materials, Vol. 9, No. 3, July 1975, pp. 216-227.

13. Monib, M.M. and Adams, D.F., "Three-Dimensional Elastoplastic Finite Element Analysis of Laminated Composites", Report UWME-DR-001-102-1, Department of Mechanical Engineering, University of Wyoming, Laramie, Wyoming, November 1980.

14. Hinton, E. and Campbell, J.S., "Local and Global Smoothing of a Discontinuous Finite Element Function Using a Least Squares Method", International Journal of Numerical Methods in Engineering, Vol. 8, pp. 461-480, 1974.

15. Goree, J.G. and Gross, R.S., "Stresses in a Three-Dimensional Unidirectional Composite Containing Broken Fibers", Journal of Fracture Mechanics, Vol. 13, No. 2, pp. 395-405, 1980.

16. Zienkiewicz, O.C., The Finite Element Method, 3rd Edition, McGraw-Hill, London (1977).

17. DiCarlo, J.A., "Mechanical and Physical Properties of Modern Boron Fibers", NASA Technical Memorandum NASA TM-73882, NASA-Lewis Research Center, Cleveland, Ohio, April 1978.

18. DiCarlo, J.A., "Predicting the Time-Temperature Dependent Axial Failure of B/Al Composites", NASA Technical Memorandum 81474, NASA-Lewis Research Center, Cleveland, Ohio, February 1980.

19. Military Handbook 5A, "Metallic Materials and Elements for Aerospace Vehicle Structure," Department of Defense, Washington, D.C., 1966.

20. Richard, R.M. and Blacklock, J.R., "Finite Element Analysis of Inelastic Structures," AIAA Journal, Vol. 7, No. 3, March 1969, pp. 432-438.

21. Behrendt, D.R., "Longitudinal Residual Stresses in Boron Fibers", Composite Materials: Testing and Design (Fourth Conference), ASTM STP 617, American Society for Testing and Materials, 1977, pp. 215-226.

22. Adams, D.F., "Micromechanical Failure Predictions for Polymer-Matrix Composites," Proceedings of the Fifth Churchill Conference on Deformation, Yield and Fracture of Polymers, University of Cambridge, Cambridge, England, March 1982.

23. Mahishi, J.M. and Adams, D.F., "Fracture Behavior of a Single-Fiber Graphite/Epoxy Model Composite Containing a Broken Fibre or Cracked Matrix", to appear in the Journal of Materials Science, Vol. 17, 1982.